

## 25. CONSOLIDATION AND STRENGTH ASSESSMENT OF DEEP-OCEAN SEDIMENTS FROM THE ARGO AND GASCOYNE ABYSSAL PLAINS, INDIAN OCEAN<sup>1</sup>

Michael Riggins<sup>2</sup>

### ABSTRACT

Twenty-one samples, ranging in depth from 0 to 150 meters below seafloor (mbsf), were obtained from Leg 123 Sites 765 and 766. All samples were tested for Atterberg limits: 14 for laboratory vane shear strength and seven for uniaxial consolidation. Based on the determined Atterberg limits, along with shipboard measurements of water content, the sediment appears to be underconsolidated from 0 to 40 mbsf at Site 765 and from 0 to 80 mbsf at Site 766. Normal consolidation trends were observed for the sediments below these depths. Vane shear strengths, when compared with calculated values for a normally consolidated clay, indicate underconsolidated sediment at both sites. However, the use of Atterberg limit and vane shear strength data to assess consolidation state is complicated by the presence of silt-sized calcium carbonate in the form of nannofossil ooze.

Thus, uniaxial-consolidation test data were analyzed to determine the overconsolidation ratios (OCR) and sediment compressibilities. OCR values were found to be less than one (underconsolidated) at both sites, using two separate methods of analysis.

### INTRODUCTION

Two sites (765 and 766) were drilled during Leg 123. Site 765, on the Argo Abyssal Plain, consisted essentially of two separate drilling operations. The first holes (765A, 765B, and 765C) involved advanced piston core (APC), extended-core barrel (XCB), and rotary core barrel (RCB) drilling and sampling operations through the sediment column and part of the way into basement rock. The second operation (Hole 765D) consisted of RCB drilling and sampling in basement basalt. Site 766, on the Gascoyne Abyssal Plain, was confined to Hole 766A, which was RCB drilled and sampled through the sediment and into basement rock.

At both sites, a complete suite of physical-properties measurements was performed on the recovered cores on board the *JOIDES Resolution* (Shipboard Scientific Party, 1990a, 1990b). These tests consisted of basic physical properties (i.e., water content, bulk density, grain density, and porosity), along with shear strength, acoustic velocity, and thermal conductivity measurements. In addition to shipboard tests, 14 subcores and seven whole-round cores were obtained for land-based determination of Atterberg limits, additional shear-strength measurements, and uniaxial consolidation tests. Note that samples came from both Sites 765 and 766 and have been limited to depths of less than 150 mbsf because of equipment limitations. The samples obtained, along with the types of tests performed, are given in Tables 1 and 2 for Sites 765 and 766, respectively.

### SEDIMENT STRATIGRAPHY

The upper 150-m interval at Site 765 consists of redeposited calcareous sediments. These calcareous sediments normally occur as graded sequences, typically with sharp, locally scoured basal contacts, and fine upward from calcareous ooze with clay to clayey nannofossil ooze. The clayey nannofossil ooze constitutes the main body of most graded sequences. The interval from 0 to

Table 1. Site 765 samples and tests performed.

Sample	Depth (mbsf)	Core	Test performed
123-765A-1H-5	7.5	Subcore	Vane shear Atterberg limits
123-765B-3H-4	24.8	Subcore	Vane shear Atterberg limits
-4H-4	34.5	Whole-round	Consolidation Atterberg limits
-5H-4	44.1	Subcore	Vane shear Atterberg limits
-7H-5	64.9	Subcore	Vane shear Atterberg limits
-8H-4	73.1	Whole-round	Consolidation Atterberg limits
-11H-5	103.5	Whole-round	Consolidation Atterberg limits
-13H-5	122.7	Subcore	Vane shear Atterberg limits
-15H-5	142.0	Subcore	Vane shear Atterberg limits

40.6 mbsf consists of redeposited clayey calcareous sediment (turbidites) having lesser amounts of clayey siliceous ooze. From 40.6 to 150 mbsf, the clayey calcareous ooze contains complex sequences made up of deformed blocks (slumps), matrix-supported intraformational conglomerates (debris flows), and graded sequences (turbidites).

Calcium carbonate content in the upper 150 m of sediment at Site 765 is highly variable and ranges from 0.3 to 81.4 wt%. This high degree of variability is attributed to the turbidite sequences, in which calcium carbonate may vary from near 80 wt% at the coarse turbiditic base to almost 0 wt% in the clay interval that characterizes the tops of these turbidites.

The upper 150 m of sediment at Site 766 consists essentially of three separate intervals. The first interval (0–82.8 mbsf) consists of a nannofossil ooze and is generally featureless and homogeneous. The second interval (82.8–114.8 mbsf) is a heterogeneous succession of nannofossil oozes, zeolitic clays, and thin, coarser, carbonate, graded sequences. The third interval (114.8–150 mbsf) is nannofossil ooze having an abundance of carbonate sequences and clays.

Calcium carbonate content in the first interval (0–82.8 mbsf) is high and varies from 62.6 to 95.8 wt%. For the second and third intervals (82.8–150 mbsf), the calcium carbonate content is highly variable and ranges from 0.3 to 90.8 wt%. This variability is associated with the higher frequency of turbidite deposition, as discussed above. From 82.8 to 150 mbsf, a general decrease in carbonate content occurs with depth.

<sup>1</sup> Gradstein, F. M., Ludden, J. N., et al., 1992. *Proc. ODP, Sci. Results*, 123: College Station, TX (Ocean Drilling Program).

<sup>2</sup> Department of Engineering, Colorado School of Mines, Golden, CO 80401, U.S.A.

**Table 2. Site 766 samples and tests performed.**

Sample	Depth	Core type	Test performed (mbsf)
123-766A-1R-1	1.5	Subcore	Vane shear Atterberg limits
-2R-4	13.8	Whole-round	Consolidation Atterberg limits
-3R-3	21.8	Subcore	Vane shear Atterberg limits
-5R-2	39.7	Subcore	Vane shear Atterberg limits
-6R-6	55.3	Whole-round	Consolidation Atterberg limits
-7R-3	60.5	Subcore	Vane shear Atterberg limits
-9R-5	82.8	Subcore	Vane shear Atterberg shear
-11R-1	96.2	Whole-round	Consolidation Atterberg limits
-11R-3	99.2	Subcore	Vane shear Atterberg limits
-13R-1	115.4	Subcore	Vane shear Atterberg limits
-14R-1	125.1	Whole-round	Consolidation Atterberg limits
-15R-5	140.7	Subcore	Vane shear Atterberg limits

## TEST PROCEDURES AND METHODS

Test procedures followed represent methods that have been standardized by the American Society for Testing and Materials (ASTM, 1989a and 1989b) or that can be found in standard references (Bowles, 1986; Boyce, 1977; Wray, 1986).

### Atterberg Limits

Atterberg limits provide an indication of the range of moisture contents over which the sediment exhibits a plastic or "clayey" behavior. The uppermost boundary, the liquid limit (LL), represents a transition from a plastic to a semi-liquid state. The lower boundary, the plastic limit (PL), represents the transition from a plastic to a semi-solid. The difference in the two values represents the plasticity index (PI), or

$$PI = LL - PL. \quad (1)$$

The higher the PI, the greater the percentage of active clay minerals present within the sediment.

Atterberg limits are often used in empirical relationships to assess the general shear-strength characteristics of a normally consolidated clay sediment and the sediment-compressibility characteristics. However, Nacci et al. (1975) noted that for silt-sized (2–10  $\mu\text{m}$  diameter) sediments, high-carbonate sediments may exhibit a water content well above that of low-carbonate sediments. This difference may be attributed to the presence of intraparticle water that exists in the hollow structure of nanofossils. This anomalously high water content for silt-sized calcareous sediments affects both the liquid and plastic limits. The presence of intraparticle water in silt-sized carbonate sediments complicates "classical" interpretations of Atterberg limits data and their use in empirical relationships. This problem can be minimized by using the plasticity index, which is unbiased by carbonate content. Even for high-carbonate sediments, the Atterberg limits serve as useful indicators when assessing general trends.

The liquid and plastic limits as well as sediment water content have been corrected to a salt concentration of 35 ppm.

### Shear Strength

Sediment shear strength was evaluated in the laboratory using a Wykeham-Farrance motorized, miniature vane-shear apparatus. This system is identical to that used on board the *Resolution*. Shear strengths were measured for each of the 14 subcore samples, which then were used to determine Atterberg limits.

### Consolidation

Consolidation tests provide information regarding the compressibility of a sediment layer resulting from the expulsion of pore water driven by an imposed load of overlying sediments. The

test performed was the standard uniaxial consolidation test. In this test, a sediment sample is confined laterally within a metal ring and then subjected to a series of incremental loads, with each load being applied for a period of 24 hr. Test data provide information concerning vertical deformation as a function of applied stress. For loading conditions (i.e., increasing applied stress), this relationship is described by the compression index ( $C_c$ ),

$$C_c = -\frac{\Delta e}{\Delta \log(P')}, \quad (2)$$

where  $\Delta e$  represents the change in void ratio for a logarithmic change in applied stress,  $\Delta \log(P')$ . For unloading or rebound conditions (i.e., decreasing applied stress and recoverable strains), the relationship is defined as the rebound index,  $C_r$ ,

$$C_r = -\frac{\Delta e}{\Delta \log(P')}. \quad (3)$$

In addition, test data provide information concerning the relative degree of consolidation, as represented by the overconsolidation ratio, OCR,

$$OCR = \frac{\sigma'_c}{\sigma'_o}, \quad (4)$$

where  $\sigma'_c$  represents the pre-consolidation stress or the maximum past pressure applied to the sediment, as determined by a graphical procedure, and  $\sigma'_o$  represents effective overburden stress, determined by the hydrostatic weight of the overlying sediments. A sediment is considered normally consolidated (i.e., all excess pore-water pressures resulting from overburden deposition have dissipated) if  $OCR \approx 1$ . An underconsolidated sediment ( $OCR < 1$ ) is one in which sufficient time has not passed, or which stratigraphy hinders the complete dissipation of excess pore-water pressures. Underconsolidated sediments are often a result of rapid deposition of sediment. A sediment is overconsolidated ( $OCR > 1$ ) if its maximum past pressure exceeds its present effective overburden stress. Overconsolidated sediments can result from surface erosion or physical and chemical reactions.

Consolidation tests were performed on seven whole-round cores. These samples also were used to determine Atterberg limits.

## SEDIMENT INDEX PROPERTIES

Sediment index properties consist of the basic physical properties measured on board the *Resolution*, along with the Atterberg limits determined as part of this study. Note that only the interval from 0 to 150 mbsf for Sites 765 and 766 was considered, as this interval represents the depth interval from which the samples were taken. The sample number, depth below seafloor, and Atterberg limits (LL, PL, and PI) for Sites 765 and 766 are given in Tables 3 and 4, respectively.

Water contents of the sediments have been plotted as a function of depth in Figure 1 for Sites 765 and 766. Also in this figure are the LL and PL, shown by "+" signs, and the PI, shown by a solid horizontal line that connects these limits.

In Figure 1A (Site 765) one can see that in the upper 40 m of sediment, the sediment water contents generally are higher than the LLs. For the interval from 40 to 150 mbsf, water contents decrease from values near the LL, down to those approaching the PL. Therefore, from this profile one might infer that the upper 40 m of sediment is underconsolidated, and normal consolidation trends can be observed with depths below 40 mbsf. This observation is consistent with sediment stratigraphy in that the interval

**Table 3. Destinations of Atterberg limits at Site 765.**

Sample	Depth (mbsf)	Atterberg limits		
		Liquid limit (%)	Plastic limit (%)	Plasticity index (%)
1H-5	7.5	80.2	34.2	46.0
3H-4	24.8	97.4	41.5	55.9
4H-4	34.5	138.0	49.3	88.6
5H-4	44.1	109.6	42.3	67.3
7H-5	64.9	87.7	41.1	46.6
8H-4	73.1	88.8	40.7	48.1
11H-5	103.5	109.2	46.4	62.8
13H-5	122.7	101.6	38.0	63.6
15H-5	142.0	83.7	37.0	46.7

**Table 4. Determinations of Atterberg limits at Site 766.**

Sample	Depth (mbsf)	Atterberg limits		
		Liquid limit (%)	Plastic limit (%)	Plasticity index (%)
1R-1	1.5	61.8	35.3	26.5
2R-4	13.9	71.9	36.3	35.6
3R-3	21.8	43.3	27.4	15.9
5R-2	39.7	61.5	33.7	27.8
6R-6	55.3	46.7	36.4	10.3
7R-3	60.5	52.5	27.1	25.4
9R-5	82.8	69.5	30.9	38.6
11R-1	96.2	45.9	24.2	21.7
11R-3	99.2	37.6	21.6	16.0
13R-1	115.4	95.7	42.7	53.0
14R-1	125.1	107.3	40.7	66.6
15R-5	140.7	95.4	39.4	56.0

from 0 to 40 mbsf consists of a redeposited clayey calcareous sediment (turbidites), and from 40 to 150 mbsf, the sediment consists of complex sequences of turbidites, slumps, and debris flows.

In Figure 1B (Site 766) one can see this same general trend. The water contents of the sediment generally are higher than the LLs for the interval from 0 to 80 mbsf. The values decrease, but remain near the LL, for the interval from 80 to 115 mbsf. From 115 to 150 mbsf, sediment plasticity increases significantly, as shown by the increase in PI; water contents approach values that are slightly higher than the PLs. Therefore, one can infer that the upper 115 m is underconsolidated, and that the lower section from 115 to 150 mbsf shows normal consolidation trends. This observation is also consistent with the sediment stratigraphy in that the

interval from 0 to 80 mbsf consists of a homogeneous nannofossil ooze; from 80 to 115 mbsf, the sediment becomes a heterogeneous succession of nannofossil oozes, carbonate sequences, and clays, and from 115 to 150 mbsf, an abundance of carbonate sequences and clays can be observed; hence, the significant increase in PI.

Note that in the previous discussion, the relationships between sediment/water content and Atterberg limits serve as indicators of consolidation trends. As stated earlier, the presence of intraparticle water in silt-sized carbonate sediments complicates classical interpretations of Atterberg limits data. Therefore, only a preliminary assessment of the underconsolidated state is possible from these data, and no inference can be made in regard to the normal

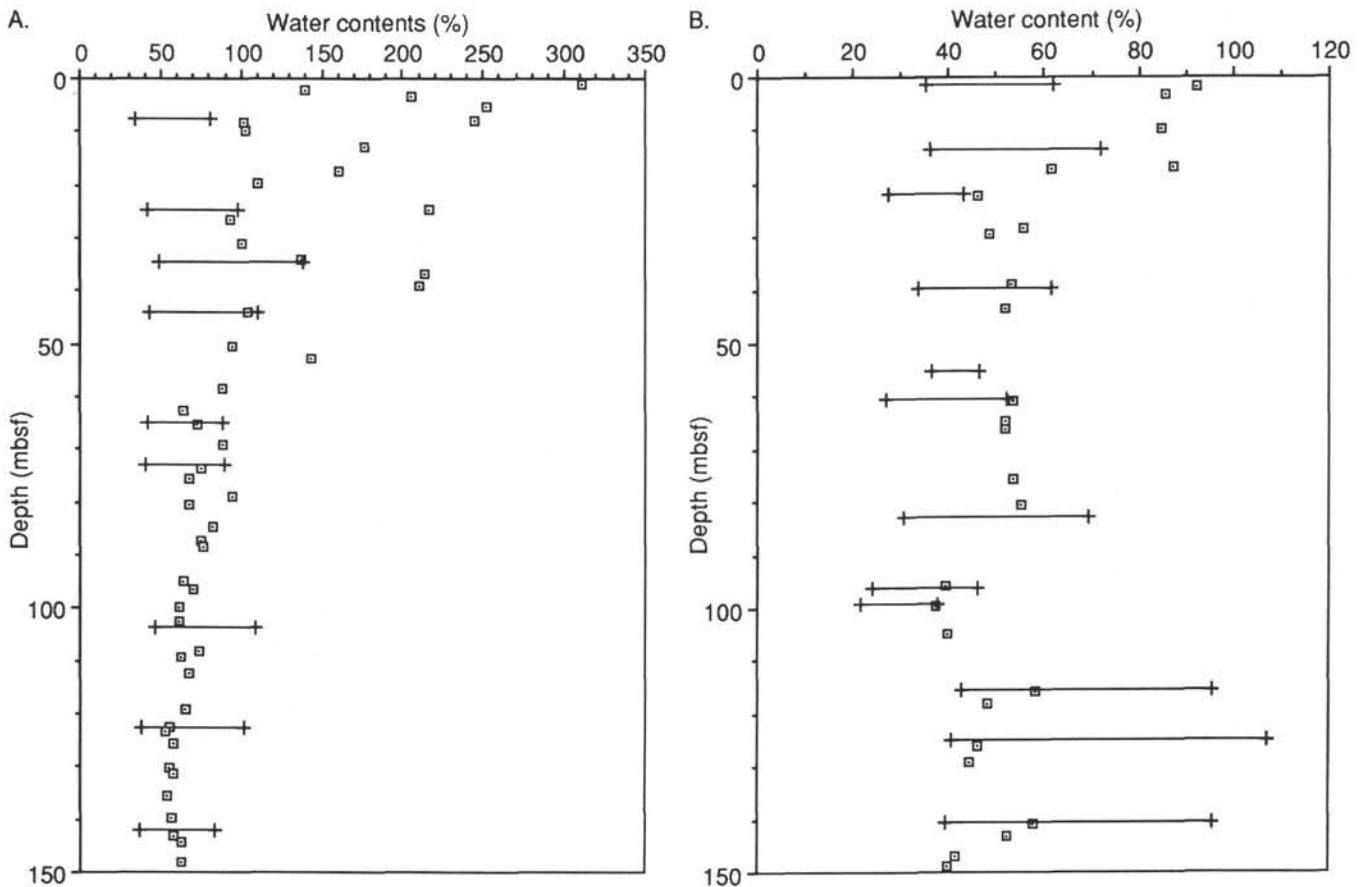


Figure 1. Water contents and Atterberg limits as a function of depth. A. Site 765. B. Site 766.

or overconsolidated states, other than normal consolidation trends that were observed. Consolidation tests will be necessary for more definitive results.

### SEDIMENT SHEAR STRENGTH PROPERTIES

In addition to the vane shear tests performed on board the *Resolution*, an additional 14 vane shear tests were performed on subcores obtained at Sites 765 and 766. The sample numbers, depths, measured vane shear strengths, and present effective overburden pressures are given in Tables 5 and 6 for Sites 765 and 766, respectively. The present effective overburden pressures were calculated on the basis of shipboard measurements of the sediment bulk density, along with a specific gravity of seawater of 1.0245.

The purpose of these additional tests was to compare measured undrained shear strengths, measured using the vane shear apparatus, with undrained shear strength values calculated using an empirical expression for normally consolidated marine clays (Bjerrum and Simons, 1960), as follows:

$$C_u/\sigma'_o = 0.11 + 0.0037 \times PI, \quad (5)$$

where PI represents the plasticity index (in percent). By comparing the normally consolidated undrained shear strength values obtained from Equation 5 with the measured values, one can gain additional information concerning the consolidation state.

The measured and calculated undrained shear strength profiles are shown in Figure 2. At both sites, calculated values for a normally consolidated clay sediment are higher than those determined on board the *Resolution* and in the laboratory. From these profiles, one might infer that the sediment at both sites is underconsolidated. However, Morgenstern (1967) found that for cemented carbonate sediments, Equation 5 predicts shear strengths that are significantly less than measured values (i.e., opposite those shown in Figure 2). A correction factor, which is a function of the percentage of calcium carbonate, was proposed. Nambiar et al. (1985) studied a carbonate clay from the West coast of India and found that the  $C_u/\sigma'_o$  ratio was independent of the percentage

of calcium carbonate present. The authors concluded that the differences in behavior could be attributed to differences in the form of the carbonate material. Here, both shipboard and shear-strength measurements were used to calculate  $C_u/\sigma'_o$  at both sites and plotted vs. the available shipboard-determined percentages of calcium carbonate (Shipboard Scientific Party, 1990c, 1990d) in Figure 3. From this figure, no apparent relationship exists between  $C_u/\sigma'_o$  and percentage of calcium carbonate for these sediments. However,  $C_u/\sigma'_o$  for Site 765 and 766 sediments may remain a function of PI, as is shown in Figure 4. Note from this figure that the measured  $C_u/\sigma'_o$  values are less than those predicted by Equation 5. Therefore, the discrepancy between the measured and predicted shear strengths might be the result of underconsolidation or might result from the presence of calcium carbonate in the form of uncemented nanofossils.

### CONSOLIDATION PROPERTIES

A series of seven consolidation tests were performed on whole-round samples obtained from both Sites 765 and 766. The test objectives were (1) to gain insight concerning the relative degree of consolidation, as expressed by the OCR, and (2) to assess the compressibility of the sediment, as determined by the compression index ( $C_c$ ).

The test results are presented as plots of void ratio ( $e$ , the ratio of void volume to volume of solids) vs. the common logarithm of the applied effective stress ( $P'$ ). The  $e$ -log( $P'$ ) plots for the samples tested are shown in Figures 5 and 6. From these figures, the preconsolidation stress was determined using Casagrande's procedure (Casagrande, 1936). This method has served as the "classical" procedure for assessing the consolidation state of terrigenous clays. The Casagrande method, which is illustrated in Figure 7A, relies on a graphical procedure to construct a bisector line at the point of maximum curvature on the  $e$ -log( $P'$ ) plot. The intersection of the bisector line with the straight line portion of the  $e$ -log( $P'$ ) plot, referred to as the virgin compression line (VCL), which represents the maximum stress that has been applied to the sediment sample, establishes the preconsolidation stress ( $\sigma'_c$ ). To check this method, a second technique, called the MGC method (Marine Geotechnical Consortium, 1985), which was developed for deep-ocean sediments, also was used. This method relies on the rebound characteristics of the sediment (Fig. 7B). A point is established on the reloading portion of the  $e$ -log( $P'$ ) curve, which is one log cycle before the point of maximum curvature. From this point, a line is drawn parallel to the rebound line until it intersects the VCL. The point of intersection establishes the preconsolidation stress ( $\sigma A'_c$ ). The samples tested, effective overburden pressure ( $\sigma'_o$ ), preconsolidation stresses ( $\sigma'_c$ ), and the resulting OCRs for both methods are presented in Table 7. One can observe from this table that the overconsolidation ratios determined by the above two methods give comparable results, with the exception of a sample from Section 123-766A-14R-1. This sample required preloading to prevent swelling during the initial loading; however, during unloading and reloading, swelling occurred (see Fig. 6D). This factor affects the MGC method, but not the Casagrande procedure. In addition, one observes from Table 7 that the upper 150 m of sediment at both sites is underconsolidated. This is indeed thought to be the case, as the sediment stratigraphy indicates rapid deposition at both sites.

The presence of significant amounts of calcium carbonate in the form of nanofossils should result in a shift in preconsolidation pressures to higher values, thus increasing the OCRs (Nacci et al., 1975). But this does not appear to be the case for those samples tested.

The  $e$ -log( $P'$ ) data (Figs. 5 and 6) also are used to calculate the compression index ( $C_c$ ) from the slope of the lower, straight-lined portion of the curves (i.e., the VCL). In addition, these data also

**Table 5. Laboratory vane shear strengths from Site 765 samples.**

Sample	Depth (mbsf)	Vane shear strength (kPa)	Effective overburden pressure (kPa)
1H-5	7.5	5.8	21.9
3H-4	24.8	18.5	97.9
5H-4	44.1	29.6	178.7
7H-5	64.9	62.0	285.1
13H-5	122.7	90.6	667.1
15H-5	142.0	68.6	825.0

**Table 6. Laboratory vane shear strengths from Site 766 samples.**

Sample	Depth (mbsf)	Vane shear strength (kPa)	Effective overburden pressure (kPa)
1R-1	1.5	6.5	8.5
3R-3	21.8	8.1	128.6
5R-2	39.7	14.6	278.1
7R-3	60.5	9.6	427.7
9R-5	82.8	94.4	592.2
11R-3	99.2	16.6	721.0
13R-1	115.4	188.2	865.9
15R-5	140.7	*	1083.2

\*No value as sample; showed cracking prior to failure.

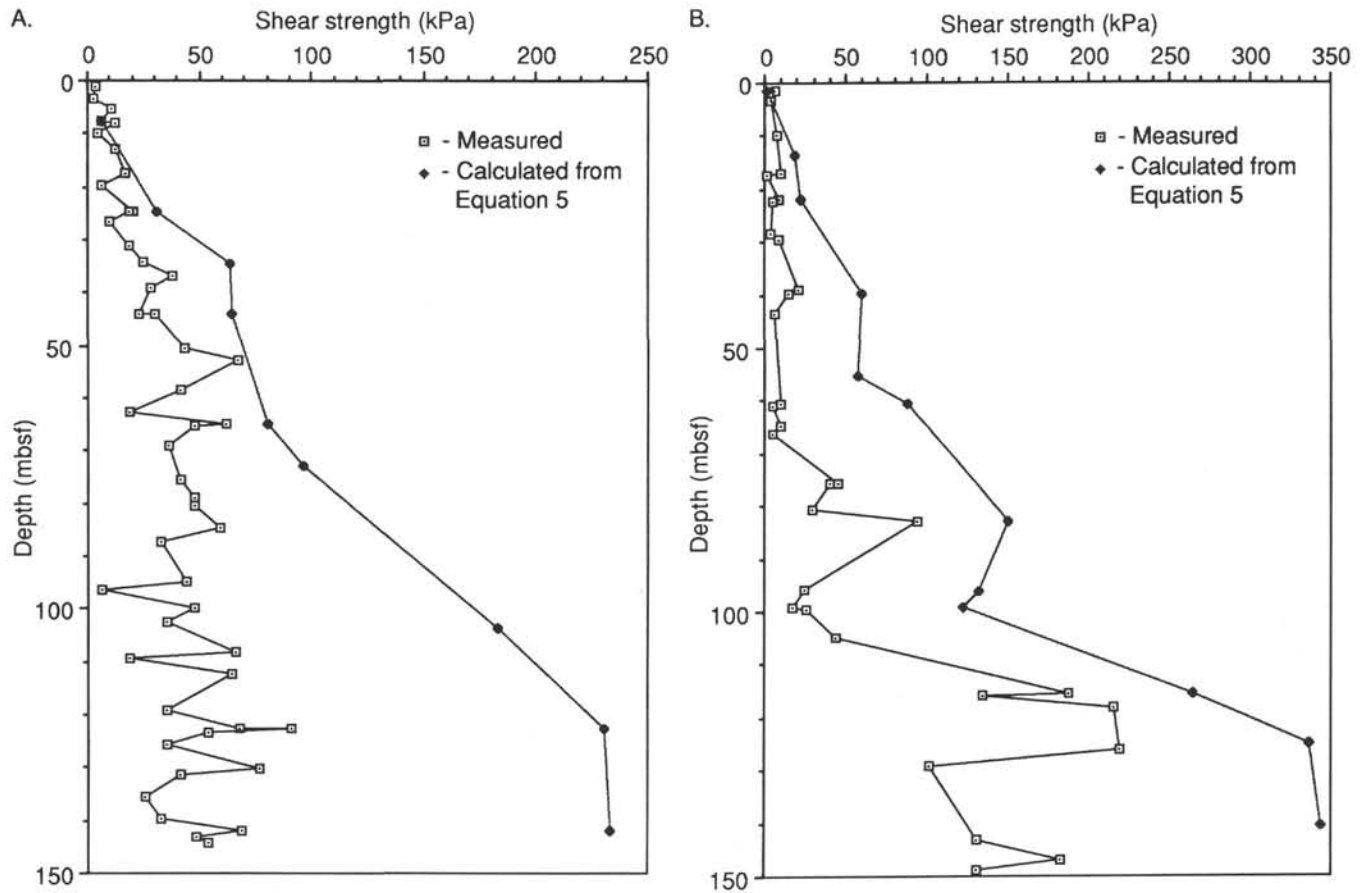


Figure 2. Sediment shear strength as a function of depth. A. Site 765. B. Site 766.

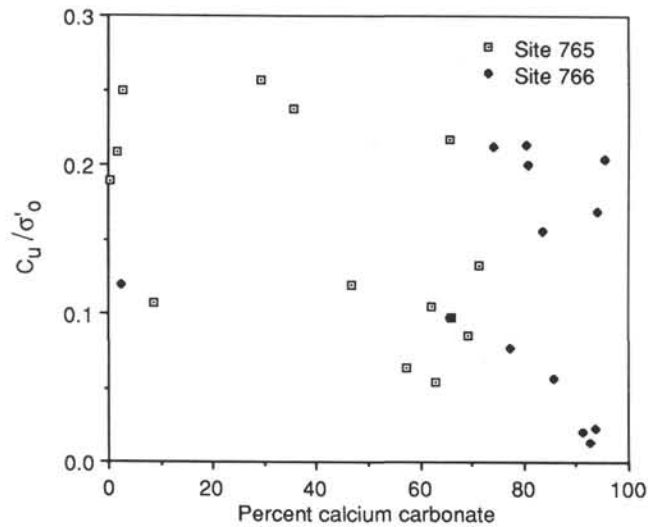


Figure 3. Ratio of sediment undrained shear strength to effective overburden pressure for difference weight percentages of calcium carbonate.

are used to calculate the slope of the unloading and reloading curves (i.e., the rebound index  $[C_r]$ ). The samples tested, along with measured compression and rebound indexes, are given in Table 8. The compression index also can be calculated using the following empirical relationship developed for calcareous sediments (Nacci et al., 1975),

$$C_c = 0.02 + 0.014 \times PI, \quad (6)$$

where PI is the plasticity index (in percent). This relationship along with the measured compression indexes are shown in Figure 8. One can see from this figure that the measured and calculated values of compression index show excellent agreement. The lone exception is the sample from Section 123-766A-14R-1 that, as described previously, required preloading to prevent initial swell.

**SUMMARY AND CONCLUSIONS**

Twenty-one samples from Leg 123 (Sites 765 and 766) obtained from depths of 0 to 150 mbsf were tested to gain additional information regarding the consolidation stress history of the sediments. All samples were used to determine Atterberg limits: 14 for vane shear strengths and seven for consolidation.

Based on a comparison of shipboard-measured water contents with Atterberg limits, one can infer that the upper section of the sediment column (0–40 mbsf, Site 765, and 0–80 mbsf, Site 766) is underconsolidated. Below this section, sediments exhibit normal consolidation trends (i.e., the water content decreases from values near the LL to those approaching the PL as a function of depth). One cannot infer normal or overconsolidation in these deeper sediments because of the presence of nanofossils and their associated effect on water contents. Vane shear strength data, when compared to calculated undrained shear strengths for a normally consolidated marine clay, as determined from sediment plasticity and effective overburden pressures, indicates that the upper 150 m of sediment at both sites is underconsolidated. However, the use of vane shear strengths as well as empirical relationships involving Atterberg limits to determine the consoli-

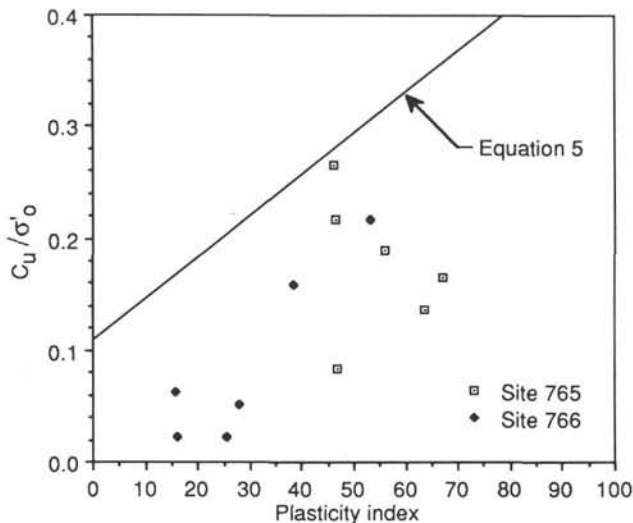


Figure 4. Ratio of sediment undrained shear strength to effective overburden pressure as a function of the measured plasticity index and those calculated from Equation 5.

ation state of calcareous sediments is currently being debated. To help resolve this issue, a series of consolidation tests were performed using three samples from Site 765 and four samples from Site 766. These data were evaluated to the pre-liquidation stresses using two separate methods, namely the Casagrande and MGC procedures. If one knows the preconsolidation stress and the effective overburden pressure, one can determine the OCR. At Site 765, OCR values ranged from 0.244 to 0.552 for the Casagrande method and from 0.337 to 0.552 for the MGC method. At Site 766, OCR values ranged from 0.261 to 0.475 for the Casagrande method and from 0.248 to 0.847 for the MGC method. In all cases, OCR values were less than one; therefore, one may conclude that the upper 150 m of sediment at both sites is under-consolidated. This conclusion is consistent with the geologic history of the area: at Site 765 numerous turbidite sequences suggest rapid deposition, and at Site 766, located at the base of Exmouth Plateau, sediment deposition is known to be rapid.

#### ACKNOWLEDGMENTS

I thank James Warner for assisting me with the laboratory tests and Robin Brereton, my fellow physical-properties specialist on board the *Resolution*. In addition, thanks to Felix Gradstein, John Ludden, Andy Adamson, and the scientific staff and crew of the

*Resolution*. I am particularly indebted to Dan Quoidbach for his special assistance in helping me obtain subcores and whole-round cores for this study.

#### REFERENCES

- ASTM, 1989a. Standard test method for liquid, plastic limit, and plasticity index of soils. In *Annual Book of ASTM Standards for Soil and Rock; Building Stones* (Vol. 4.08): Philadelphia (American Society for Testing of Materials), D 4318-84:769-784.
- \_\_\_\_\_, 1989b. Standard test method for one-dimensional consolidation properties of soils. In *Annual Book of ASTM Standards for Soil and Rock; Building Stones* (Vol. 4.08): Philadelphia (American Society for Testing of Materials), D 2435-80:390-396.
- Bjerrum, L., and Simmons, N. E., 1960. Comparison of shear strength characteristics of normally consolidated clays. In *Res. Conf. on Shear Strength of Cohesive Soils*: New York (Am. Soc. Civ. Eng.), 711-726.
- Bowles, J. E., 1986. *Engineering Properties of Soil and Their Measurement* (3rd ed.): New York (McGraw-Hill).
- Boyce, R. E., 1977. Deep Sea Drilling Project procedures for shear strength measurement of clayey sediment using modified Wykeham Farrance laboratory vane apparatus. In Barker, P., Dalziel, I.W.D., et al., *Init. Repts. DSDP*, 36: Washington (U.S. Govt. Printing Office), 1059-1068.
- Casagrande, A., 1936. Determination of preconsolidation load and its practical significance. *Proc. 1st Conf. Soil Mech. Found. Eng.* (Vol. 3): Cambridge, MA (Am. Soc. Civ. Eng.), 60-64.
- Marine Geotechnical Consortium, 1985. Geotechnical properties of northwest Pacific pelagic clays: Deep Sea Drilling Project Leg 86, Site 576 A. In Heath, R. C., Burckle, L. H., et al., *Init. Repts. DSDP*, 86: Washington (U.S. Govt. Printing Office), 723-758.
- Morgenstern, N. R., 1967. Submarine slumping and the initiation of turbidity currents. In Richards, A. F. (Ed.), *Marine Geotechnology: Urbana* (Univ. Illinois Press), 189-220.
- Nacci, V. A., Wang, A. M., and Demars, K. R., 1975. Engineering behavior of calcareous soils. In *Civil Engineering in the Oceans III* (Vol. 1). Am. Soc. Civ. Eng., 380-400.
- Nambiar, M.R.M., Rao, G. V., and Gulhati, S. K., 1985. The nature and engineering behavior of fine-grained carbonate soil from off the West coast of India. *Mar. Geotechnol.*, 6:145-171.
- Shipboard Scientific Party, 1990a. Site 765. In Ludden, J. N., Gradstein, F. M., et al., *Proc. ODP, Init. Repts.*, 123: College Station, TX (Ocean Drilling Program), 63-267.
- \_\_\_\_\_, 1990b. Site 766. In Ludden, J. N., Gradstein, F. M., et al., *Proc. ODP, Init. Repts.*, 123: College Station, TX (Ocean Drilling Program), 269-352.
- Wray, W. K., 1986. *Measuring Engineering Properties of Soils*: Englewood Cliffs, NJ (Prentice-Hall).

Date of initial receipt: 30 May 1990

Date of acceptance: 22 May 1991

Ms 123B-133

Table 7. Consolidation stress history, Sites 765 and 766.

Sample	Depth (mbsf)	$\sigma'_v$ (kPa)	Casagrande method		MGC method	
			$\sigma'_c$ (kPa)	OCR	$\sigma'_c$ (kPa)	OCR
123-765B-4H-4	34.5	145.0	80	0.552	80	0.552
-8H-4	73.1	333.2	170	0.510	170	0.510
-11H-5	103.5	533.7	130	0.244	180	0.337
-2R-4	13.8	76.5	20	0.261	19	0.248
-6R-6	55.3	391.2	150	0.383	170	0.435
-11R-1	96.2	694.4	330	0.475	310	0.446
-14R-1	125.1	944.6	440	0.466	800	0.847

Table 8. Compression and rebound indexes at Sites 765 and 766.

Sample	Depth (mbsf)	$C_c$	$C_r$
123-765B-4H-4	34.5	1.34	0.20
-8H-4	73.1	0.67	0.11
-11H-5	103.5	0.84	0.27
123-766A-2R-4	13.8	0.59	0.05
-6R-6	55.3	0.25	0.02
-11R-1	96.2	0.39	0.05
-14R-1	125.1	0.39	0.14

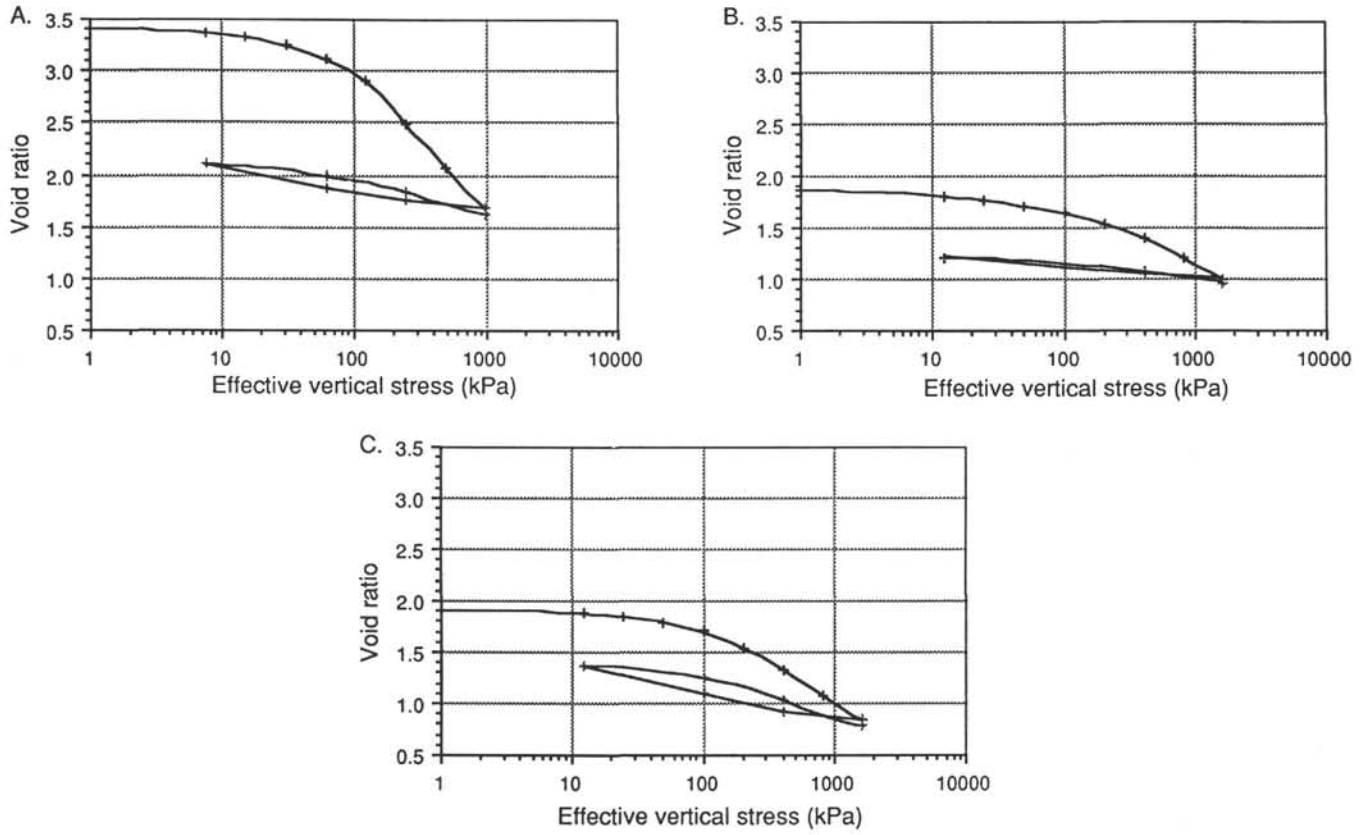


Figure 5. Plots of void ratio vs.  $\log(P')$  for samples from Site 765. **A.** Section 123-765B-4H-4 (34.5 mbsf). **B.** Section 123-765B-8H-4 (73.1 mbsf). **C.** Section 123-765B-11H-5 (103.5 mbsf).

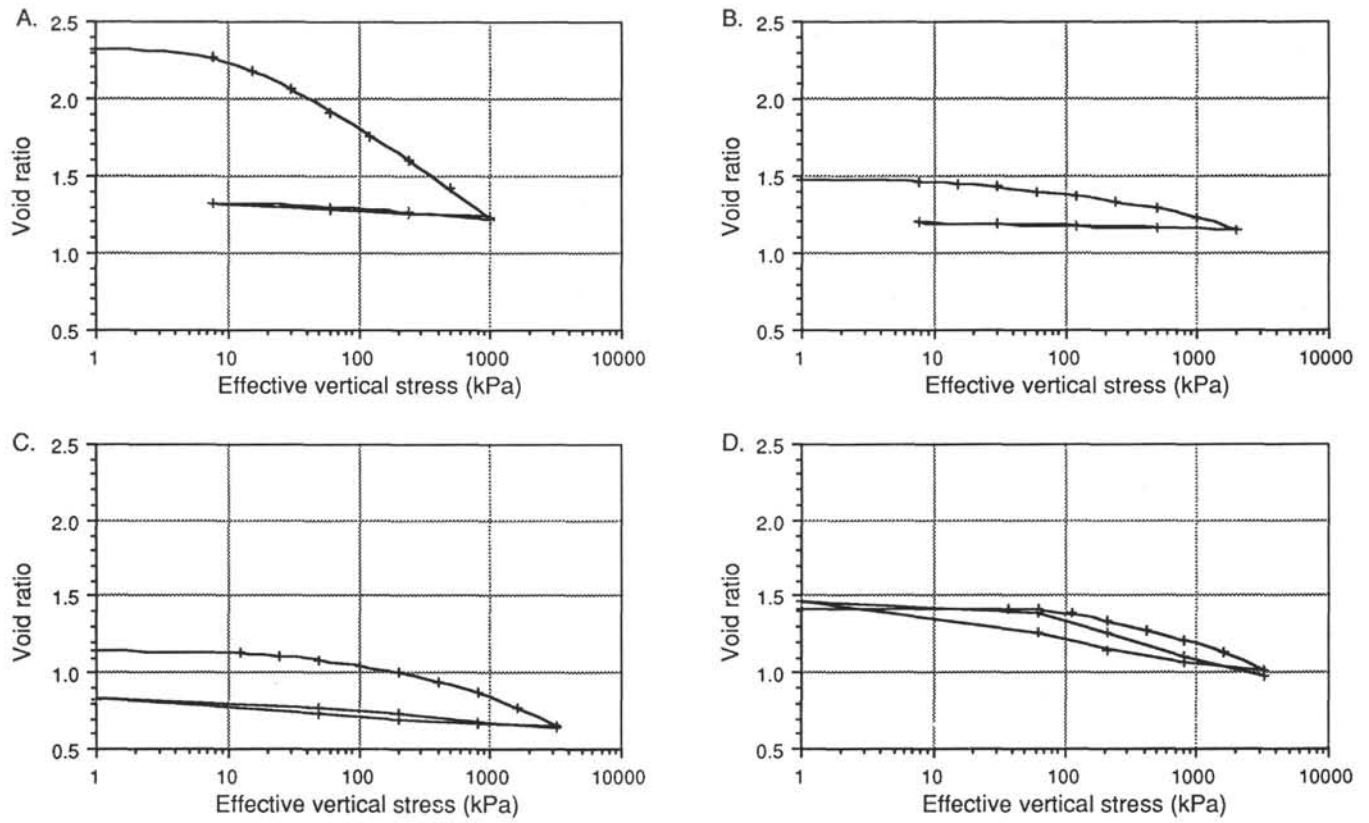


Figure 6. Plots of void ratio vs.  $\log(P')$  for samples from Site 766. **A.** Section 123-766A-2R-4 (13.8 mbsf). **B.** Section 123-766A-6R-6 (55.3 mbsf). **C.** Section 123-766A-11R-1 (96.2 mbsf). **D.** Section 123-766A-14R-1 (125.1 mbsf).

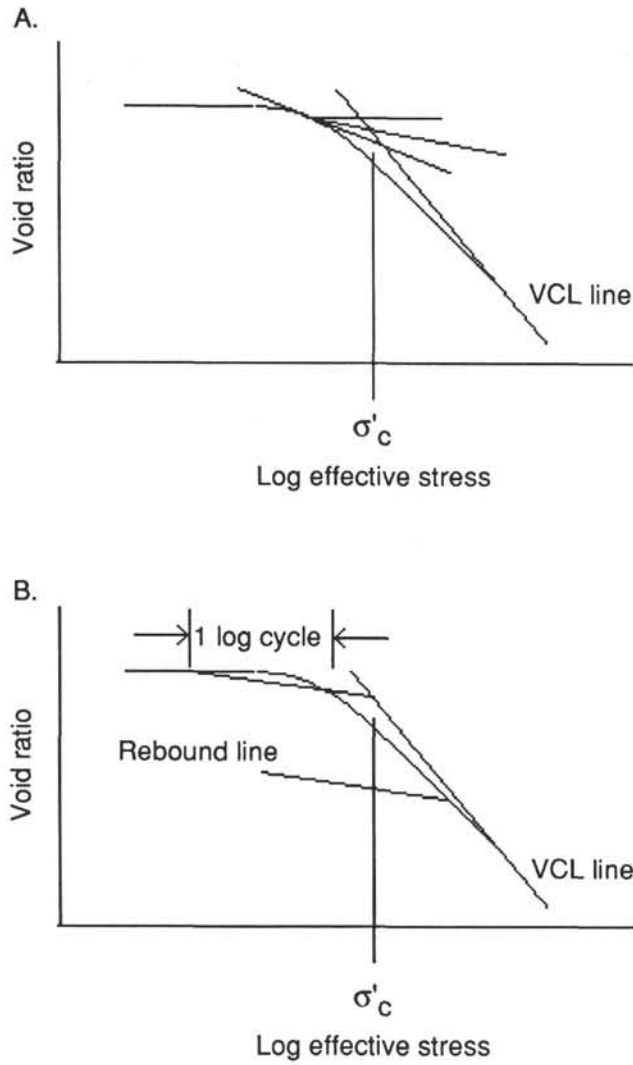


Figure 7. Methods for determining preconsolidation stress. **A.** Casagrande method. **B.** MGC method.

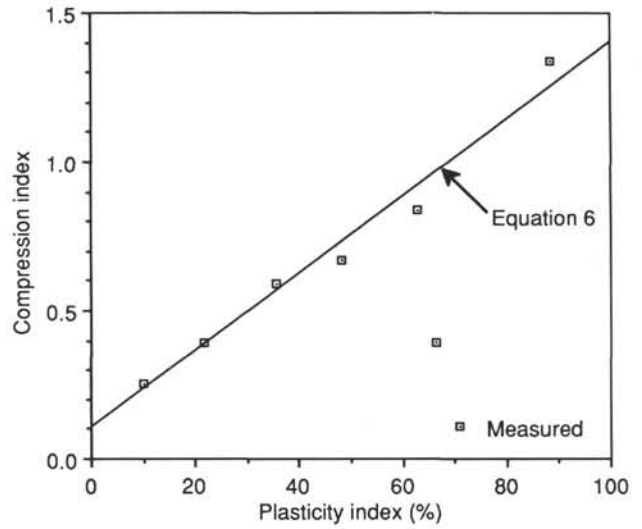


Figure 8. Measured and calculated compression index as a function of the plasticity index.